Peter Y, Comellas A, Levantini E, Ingenito EP, Shapiro SD.. Epidermal growth factor receptor and claudin-2 participate in A549 permeability and remodeling: implications for non-sma...

ARTICLE *in* MOLECULAR CARCINOGENESIS · JUNE 2009

Impact Factor: 4.81 · DOI: 10.1002/mc.20485 · Source: PubMed

5 AUTHORS, INCLUDING:

Alejandro P Comellas
University of Iowa
52 PUBLICATIONS **846** CITATIONS
SEE PROFILE

Elena Levantini
Boston Children's Hospital
26 PUBLICATIONS **846** CITATIONS
SEE PROFILE

Edward P Ingenito
Partners HealthCare
143 PUBLICATIONS **5,148** CITATIONS
SEE PROFILE

Steven D Shapiro
University of Pittsburgh
291 PUBLICATIONS **23,340** CITATIONS
SEE PROFILE

Published in final edited form as:
Mol Carcinog. 2009 June ; 48(6): 488–497. doi:10.1002/mc.20485.

Epidermal Growth Factor Receptor and Claudin-2 Participate in A549 Permeability and Remodeling: Implications for Non-Small Cell Lung Cancer Tumor Colonization

Yakov Peter[1,*], **Alejandro Comellas**[2], **Elena Levantini**[3], **Edward P. Ingenito**[1], and **Steven D. Shapiro**[4]

[1]Division of Pulmonary and Critical Care Medicine, Brigham and Women's Hospital and Harvard Medical School, Boston, Massachusetts

[2]Division of Pulmonary and Critical Care, Feinberg School of Medicine, Northwestern University, Chicago, Illinois

[3]Department of Hematology and Oncology, Beth Israel Deaconess Medical Center and Harvard Medical School, Boston, Massachusetts

[4]Department of Medicine, University of Pittsburgh, Pittsburgh, Pennsylvania

Abstract

Tumor colonization involves changes in cell permeability and remodeling. Paracellular permeability is regulated by claudins, integrated tight junction (TJ) proteins, located on the apicolateral portion of epithelial cells. Epidermal growth factor (EGF) was reported to modify cellular claudin levels and induce remodeling. To investigate a role for EGF receptor (EGFR) activation in tumor colonization we studied the effect of EGF and claudin-2 overexpression on permeability and cell reorganization in the human A549 non-small cell lung cancer (NSCLC) cell line. Our data demonstrated that A549 cells possess functional TJs and that EGF treatment increased levels of claudin-2 expression by 46%. Furthermore, EGFR signaling reduced monolayer permeability to choline and triggered cellular remodeling. The mitogen-activated protein kinase inhibitor PD98059 blocked the effect on A549 permeability and remodeling. EGF stimulation also exacerbated a fourfold increase in cell colonization elicited by claudin-2 upregulation. Our findings are consistent with the hypothesis that EGFR signaling plays an important role in A549 cell physiology and acts synergistically with claudin-2 to accelerate tumor colonization. Understanding the influence of EGF on A549 cell permeability and reorganization will help shed light on NSCLC tumor colonization and contribute to the development of novel anti-cancer treatments.

Keywords

EGF; claudin-2; A549; colonization; permeability

INTRODUCTION

Metastatic outgrowth is preceded by tumor angiogenesis and colonization. Whereas angiogenesis has been demonstrated to be induced by a plethora of cytokines, colonization is

*Correspondence to: Department of Cell Biology, Yeshiva University, 500 W 185th St, New York, NY 10033.
Yakov Peter's present address is Department of Cell Biology, Yeshiva University, New York, NY 10033.

thought to be accomplished by clonally dominant cell populations independent of exogenous growth factors [1]. Both processes require changes in cell permeability and migration [2,3].

Epidermal growth factor (EGF) is an important angiogenic factor shown to stimulate cell proliferation and invasion [4,5]. EGF downstream activation of MAP kinase (MAPK) has been shown to influence cell permeability by modification of paracellular selectivity [6–8]. These data indicate a link between EGF receptor (EGFR) activation and cell growth and permeability. This relationship is greatly emphasized as evidenced by juxtacrine activation of the EGFR [9,10] and EGF autocrine ligand-receptor activation [11]. The former involves a membrane-anchored EGFR ligand shown to modify cell barrier properties, while the latter entails EGF secreted on the basal side of cells, permeating through, and activating EGFRs on the apical surface [12,13]. Both processes occur following stimuli or damage to the epithelial monolayer.

Transepithelial permeability involves two disparate pathways. The transcellular pathway is active and engages protein-mediated transport, while the paracellular pathway is regulated by diffusion through tight junctions (TJs) at the lateral portion of adjacent epithelial cells. Claudin proteins constitute the TJ and their combinations and stoichometry confer molecular selectivity to the paracellular pathway [14–16]. Structurally, claudins possess extracellular residues that face outward, allowing them to interact with residues from neighboring adjacent cells and intracellular binding domains that modulate intra-cellular interactions [17,18]. Claudin expression is diverse both between and within tissues with lung type II-derived alveolar epithelial cells (AECs) reported to express claudins -3, -4, -5, -7, and -18 [19–21] and Madin Darby Canine Kidney (MDCKII) cell type II, derived from the distal tubule of the nephron, expressing a battery of claudins including -1, -2, -3, -4, -6, -7 [22,23]. Of these, claudin-2 has been shown to form a cation-selective TJ channel significantly reducing the transepithelial resistance (TER) of tight epithelial barriers [23–25].

The human lung A549 cell is a non-small cell lung cancer (NSCLC) line that carries a wild-type EGFR pathway. A549 cells readily proliferate to form a leaky barrier in culture [26] with the repertoire and effect of claudin dysregulation on permeability unknown. Moreover, while manifestations of cancer include tumor leakiness and claudin dysregulation, the impact of EGF autocrine ligand-receptor activation in tumor colonization has not been elucidated. In this study we investigate the role of EGF pathway stimulation on A549 cell growth and its impact on claudin-2-derived permeability.

MATERIALS AND METHODS

Generation and Maintenance of Cell Lines

Claudin-2 was cloned from a human kidney cDNA library (Clontech, Palo Alto, CA) using the 5′ forward ATGGCCTCTCTTGGCCTCCAA and TCACACATACCCTGTCAGGCT reverse primers. The resulting sequence (conformed to gene bank accession number NM 020384) was cloned into the pIRES-Hyg expression vector. A549 and MDCKII cells were then transfected with lipofectamine 2000 (GIBCO, Grand Island, NY) and selected the following day with 500 μg/mL Hygromycin B. Individual cells were then plated at a concentration of 1 cell/well in a 96-well dish. Upon confluency, clones were trypsinized and stable cell lines were grown. All cell lines were grown at 37°C, in a 10% CO_2 incubator in Dubelco's modified Eagle's medium (DMEM; GIBCO) + 10% fetal bovine serum (Hyclone, Logan, UT) with or without 500 μg/mL Hygromycin B (A.G. Scientific, San Diego, CA). For remodeling studies 1×10^5 A549 cells were plated in a 6-well dish and treated the following day with vehicle, EGF (Invitrogen, Carlsbad, CA, 200 ng/mL) or EGF + PD98059 (Sigma, St Louis, MO, 50 μM). Twenty-four hours after treatment, cells were fixed with four designated areas of each well photographed for analysis. Cell counts were carried out by an independent observer. For colonization studies we used a modified version of the two-chamber assay [27] where confluent

cell layers on a 0.4 μm porous transwell insert (3460; Corning, Corning, NY) were incubated in the upper compartment of a culture chamber. The chamber was filled to capacity with the media level sufficiently high that cells that detach could move in fluid phase to colonize the lower chamber. After 3 d the number of cells attached to the lower surface was counted.

Western Analysis and Immunofluorescence

Cells were rinsed in cold PBS, solubilized in boiling SDS sample buffer, supplemented with protease inhibitors (Protease inhibitor cocktail, Sigma), sheared through a 20 g syringe needle, and spun at 13 000*g* for 30 min. Western blots were performed as previously reported [28]. In short, proteins were quantified (DC Protein Assay; Biorad, Hercules, CA) and 70 μg of total protein was loaded onto a 10% SDS–PAGE gel, transferred onto a nitrocellulose membrane, probed, and detected by the enhanced chemiluminescent (ECL, Amersham Biosciences, Buckinghamshire, England) reaction and exposure to X-ray film. Horseradish peroxidase conjugated secondary antibodies were goat anti-rabbit and goat anti-mouse (Biorad). Primary antibodies included rabbit anti-claudin -1, -2, -4, and -5, rabbit anti-ZO1 and mouse anti-occludin (Zymed, San Francisco, CA), and monoclonal anti-actin clone AC-40 (Sigma). For immunofluorescence, cells were grown on filters, rinsed in PBS, fixed in 1% PFA, and stained using cyanine-2 goat anti-mouse and cyanine-3 conjugated affinity purified goat anti-rabbit (Jackson Immunoresearch Laboratories, West Grove, PA).

Transepithelial Resistance and Tracer Flux Studies

All physiological experiments were conducted on three separate clones for each cell line, with 2×10^5 cells plated on 0.4 μm, 12 mm diameter transwell inserts (Costar 3460) and, unless indicated, allowed to grow for 3 wk. The fact that A549 cells were plated at a low density reduced multilayering even at 3 wk in culture, however vertical outgrowths did occur. TER measurements were performed using Millicell-ERS with chopstick electrodes (Millipore, Bedford, MA) at 37°C and TER values were calculated by subtracting the contribution of the bare filter and medium and multiplying by the surface area of the insert (ohm × cm^2). Unless noted, all chemicals were purchased from Sigma. Ca^{++} depletion studies were conducted on cells growing on transwell inserts by replacement of growth media (DMEM + 10% FBS) in the basal compartment with minimal essential medium without calcium (S-MEM, GIBCO). Cells were grown for 1 wk and repleted with growth media for TER measurements. After experimentation, monolayer integrity was verified by an additional TER measurement. Permeability studies were performed in DMEM with 10 μM ^{14}C-mannitol, ^{14}C-ethanolamine, or ^{14}C-choline (Amersham, Arlington Heights, IL) added to the basal or apical solution at 37° C for 60 min. At the end of the experiment, the apical or basal solution was collected respectively and added to scintillation fluid (Ultima Gold, Parkard, Palo Alto, CA) and counted (Beckman Coulter LS 6500). Permeability experiments performed in the cold were performed as previously mentioned with radioisotope application to the apical compartment, incubation at 4°C and media collection after 1 h.

Photographic Capturing, Quantification, and Statistical Analysis

Photographs were captured using a Leica DMLB fluorescent (Bannockburn, IL) or Nikon T-3200 confocal microscope (Nikon Image Center at the Harvard Medical School). Protein quantification was performed using Scion Image (4.0.3.2, Scion Corporation, Frederick, MD). Statistical analysis was performed using Student's *t*-test for normally distributed data and non-parametric Wilcoxon rank sum test for skewed data. Data are presented as mean ± standard error of the mean (SEM).

RESULTS

EGF Stimulates MAPK to Induce A549 Cell Reorganization

The EGF cascade is active in cell growth, turnover, and epithelial to mesenchymal transition EMT [5,29,30]. We investigated the effect of EGF on A549 cell growth (Figure 1A). A549 cells generally proliferate radially to form a cobblestone pattern of adjoining cells. EGF treatment alters this pattern manifested as detachment and reorganization, whereas vehicle-treated A549 cells showed no morphological differences from controls. We quantified the percentage of cells withdrawn from clusters. The percentage of detached cells was 9.1 ± 2.1 and 62.3 ± 9.7 per microscopic field for control and EGF-treated A549 cells, respectively ($P < 0.001$). In contrast, in the MDCKII line, while a slight detachment of cells was observed, the EGF effect on reorganization was not as pronounced ($P > 0.05$; Figure 1B). Many of the phenotypic effects of EGF treatment are mediated by MAPK. To test if A549 remodeling is mediated by MAPK activation we pretreated A549 cells with PD98059, a MAPK inhibitor [31]. As seen in Figure 1C, PD98059 reverses EGF-induced A549 cell reorganization ($P < 0.05$).

To verify the involvement of MAPK in cell rearrangement we performed an immunoblot on EGF treated A549 cell extracts. As seen in Figure 2, EGF increased levels of phosphorylated MAPK ($n = 5$). As measured by densitometry, this increase was 86% higher than controls and inhibited by PD98059. To investigate if A549 cell remodeling represents an early stage of transition between epithelial and mesenchymal lineages we stained for the epithelial E-cadherin and mesenchymal alpha-smooth muscle actin proteins. Levels of the epithelial cell adhesion protein E-cadherin decreased by 34% ($n = 3$), while alpha-smooth muscle actin expression remained undetectable (data not shown). These data imply that EGF stimulation confers a distinct remodeling phenotype to A549 cells marked by elevated MAPK and a reduction of E-cadherin levels.

Convoluted Growth and Claudin-2 Expression in A549 Cells

To test if EGFR activation confers an effect on A549 physiology we needed to demonstrate the existence of TJ machinery. Claudins, occludin, and the scaffold protein ZO1 were previously shown to be critical components of the TJ [32,33]. We found lateral localization of occludin, ZO1, and claudin-2 in A549 cells (Figure 3). With reference to occludin, claudin-2 peripheral staining (Figure 3A and B) was more diffused than that of ZO1 (Figure 3C). Also the A549 layer was characterized by periodic cellular upgrowths accompanied by subcellular growth (Figures 3A and B). However, in addition, we revealed that A549 cells form dome structures seen as detachment from the substratum, with no underlying growth. These findings indicate that TJ proteins line the lateral portion of A549 cells with domes and bilayers maintaining intercellular connectivity through TJ contacts. Taken together, our findings indicate that TJ proteins line the lateral portion of A549 cells.

A549 Cells Form a Unique Semipermeable Barrier

We characterized the seal of confluent A549 and MDCKII cells and found that both are leaky with regards to TER at 43.0 ± 1.2 Ωcm^2 and 59.1 ± 1.5 Ωcm^2, respectively. It is known that Ca^{++} ions maintain TJ integrity and absence of Ca^{++} eliminates TER. Repletion of Ca^{++} reportedly triggers an overshoot of TER, known as a Ca^{++} spike, that subsides following TJ reorganization [33–35]. To investigate the impact of the TJ on A549 physiology we tested the capacity of this cell line to generate a Ca^{++} spike. We found that in the absence of basal Ca^{++}, A549 cells showed a robust twofold decrease in TER after 1 wk (Figure 4; time 0). Following Ca^{++} repletion, a fourfold increase in TER was observed after 2 h with epithelial resistance reaching 69.3 ± 1.8 Ωcm^2. At this time point TER was over 87% higher than non-treated A549 cells ($P < 0.01$), with values returning to control after 24 h (Figure 4). These data

indicate that A549 barrier sealing is Ca^{++} dependent. Next we proceeded to investigate the permeability properties of A549 cells. Ethanolamine (MW 61), choline (MW 121), and mannitol (MW 182) are important molecular tracers commonly used in permeability studies. In Figure 5, basal-to-apical ethanolamine permeability through the A549 layer was 23.4 ± 2.6 μm/(M hr cm^2). These values are similar to basal-to-apical ethanolamine flux through MDCKII cells 20.1 ± 1.1 μm/(M hr cm^2). In contrast, permeability to mannitol is fourfold higher in A549 than MDCKII cells at 28.2 ± 1.9 and 5.9 ± 3.2 μm/(M hr cm^2), respectively ($P < 0.05$). As mannitol was previously shown to be occluded from the MDCKII TJ [14], A549 pores seem to be of larger magnitude to accommodate mannitol and choline flux (data not shown). Interestingly, mannitol (the largest molecule of the three) diffusion occurs at increased rates contrary to that expected based upon size alone, reflecting complex specificity of the A549 barrier.

To investigate if mannitol permeability takes place through transcellular mechanisms, we repeated our experiments at 4°C. Incubation of cells at this temperature are known to reduce paracellular diffusion and obliterate active transport. We examined the influence of temperature on A549 cellular flux. As seen in Figure 5, while ethanolamine permeability did not change, mannitol permeability significantly decreased from 28.2 ± 1.9 to 10.6 ± 1.9 μm/(M hr cm^2) ($P < 0.01$) corresponding with a fraction of active transport. To clarify a role for specialized transport we sought to establish a direction to tracer movement, namely toward the basal or apical compartments (Figures 5A and B). Mannitol permeability did not show any net differences, however ethanolamine preferentially diffused in the apical to basal direction. Taken together, these data indicate formation of a Ca^{++} dependent A549 barrier regulated in addition by protein-mediated transport mechanisms.

EGF Treatment Elevates Levels of Claudin-2 and Modifies Permeability in A549 Cells

In previous studies, EGF stimulation has been shown to influence claudin expression with the subsequent effect on epithelial physiology differing between cell types [8,19,36]. We found that A549 cells express occludin and claudin-2 but not -1, -4, and -5 (data not shown). To test the effect of EGF on claudin-2 expression we treated A549 cells and performed immunoblots on total cell extracts. EGFR activation elevated claudin-2 expression by an average of 46% (Figure 6; $n = 3$). We then examined the influence of EGF on A549 TER and permeability. While no differences in TER were observed after 1.5 h, basal-to-apical permeation of choline significantly decreased from 4.5 ± 0.1 to 4.1 ± 0.1 μm/(M hr cm^2) with $P < 0.05$. PD98059 inhibited the reduction in choline flux and reversed the EGF effect on permeability. Vehicle-treated cells showed no differences from controls. These data indicate that EGF influences claudin-2 expression and subsequently affects A549 layer permeability.

Claudin-2 Upregulation Affects A549 Cell Permeability

These results prompted us to investigate a relationship between claudin-2 and EGF. Specifically, we tested if elevated claudin-2 levels interfere with the EGF phenotype observed in A549 cells. Accordingly, we cloned and overexpresssed human claudin-2 in A549 and MDCKII cells (Figure 7). Transfected A549 and MDCKII cell lines ($n = 3$) show an 8.8- and 10.3-fold increase in claudin-2 levels as compared to A549 (A549-con) and MDCKII empty vector controls, respectively ($P < 0.05$). In both cell lines no differences in TER were observed between controls and claudin-2 overexpressing clones. We then tested if upregulation of claudin-2 would influence A549 permeability. A significant 28% increase in basal-to-apical ($P < 0.05$; Figure 5A) but not apical-to-basal ethanolamine flux was observed in claudin-2 overexpressing A549 cells (A549-Cl2) with ethanolamine permeability at 4°C not altered. A549-Cl2 mannitol permeability showed a statistically significant 37% and 36% increase in basal-to-apical and apical-to-basal permeabilities respectively ($P < 0.01$ and $P < 0.05$; Figure 5B), that was significantly reduced at 4°C ($P < 0.001$). An opposite trend was observed in

MDCKII cells where claudin-2 upregulation induced a 32% *reduction* of ethanolamine permeability as compared with controls ($P < 0.001$; data not shown). These data indicate that claudin-2 upregulation specifically modifies A549 flux with no effect on TER.

EGF Exacerbates Claudin-2-Induced A549 Colonization

Our data indicate that EGF signaling induces cell reorganization, while claudin-2 upregulation increases cell permeability in the A549 cell line. Meanwhile, previous reports showed a link between EGF signaling and the colonization of mammary tumor cells [37]. We investigated the effect of EGF and claudin-2 upregulation alone, and their combined effect on A549 cell colonization using a modified version of the two-chamber assay [38]. This model measures the capacity of cells to migrate, adhere, and repopulate the lower compartment of a transwell dish. Our findings show that EGF alone did not influence colonization of the control cell lines (Figure 8). However, claudin-2 overexpression increased A549 colonization from $4.7 \pm 1.7 \pm 10^3$ to $21.2 \pm 3.3 \pm 10^3$ cells in the lower compartment (Figure 8). Thus, A549-Cl2 elicited over a fourfold increase in colonization as compared with A549-con ($P < 0.01$). EGF exacerbated A549-Cl2 colonization increasing it twofold ($P < 0.05$) with values over eightfold higher than controls ($P < 0.001$). Preincubation of A549-Cl2 cells with PD98059 reversed the EGF effect ($P < 0.05$). To assess if cell colonization progresses by way of the porous insert we performed sections through the transwell filter. Cell migration or haptotaxis did not occur through the filter holes as the inferior portion of the insert was devoid of cells (data not shown). In summary, claudin-2 upregulation increases A549 cell colonization that is further enhanced by EGF treatment.

DISCUSSION

There is accumulating evidence that EGF signaling influences cell growth and remodeling. In this study we investigated a link between EGFR activation and cell permeability differences on A549 growth and colonization. We report that EGF induces A549 cellular reorganization and modifies permeability via MAPK mediation. In turn, EGF also upregulates claudin-2 that alone modifies A549 permeability and colonization. Finally, the combination of claudin-2 overexpression and EGF stimulation is synergistic in A549 colonization.

AECs have been reported to possess fluid transport with large solutes shown to escape at higher rates than smaller molecules [39,40]. We report that the human A549 cell line forms a functional and semi-permeable barrier with similar properties. Trans-differentiating AECs form domes in culture and show claudin expression patterns, with the exception of claudin-2, that correspond to our data [19]. Others have shown that A549 cells preserve other critical proteins involved in alveolar fluid absorption [41]. These data indicate that A549 cells, in addition to serving as a model for NSCLC, retain many physiological properties of AECs. The A549 barrier may provide insight to ongoing studies of permeability, including those investigating the lung as an avenue for stem cell delivery [42].

We show that EGFR activation mediated through MAPK triggered A549 cell reorganization and increased levels of claudin-2 to affect cellular permeability. Our data correspond with previous studies reporting that MAPK was necessary during early phases of lung morphogenesis and tumor angiogenesis [43,44]. MAPK was also shown to convey migration and invasive properties to MDCK cells [45] and was required for claudin-2 mediated formation of the TJ in a human colon cancer cell line [46]. Thus, we conclude that MAPK constitutes a beneficial sensor conveying input originating from EGFRs and TJs at the plasma membrane.

Our data suggest that A549 adenocarcinoma cells laterally express the TJ proteins occludin, claudin-2, and ZO1 to form a functional, yet leaky, cellular barrier. Endogenous expression of claudin-2 in A549 cells has not been reported previously and may account for the leaky

properties of this cell line, as claudin-2 was shown to reduce the TER of MDCKI cells more than 20-fold [25]. We show that claudin-2 upregulation does not affect A549 TER but increases cell permeability. A leaky barrier may contribute to metastasis enhancing tumor remodeling by increasing the uptake of nutrients and growth factors. Defects resulting from claudin-2 overexpression would correlate well with data concerning claudin dysregulation in several cancer cells [16,47]. Therefore, we suggest that claudin-2 expression is an important identifier of the A549 cancer phenotype contributing to both permeability and colonization. Accordingly, claudin-2 may serve as an important marker of NSCLC in tumor biopsies.

Epithelial sheaths form a semipermeable barrier that regulates EGF autocrine ligand receptor activation. Claudin expression patterns convey selectivity to TJ pores with upregulation eliciting changes in several cell types [25,48]. We found that overexpression of the low-resistant claudin-2 did not affect TER in either A549 or MDCKII cells and concurred with findings from others studies [23]. However, the increase in A549-Cl2 paracellular flux and colonization is significant. Meanwhile, EGF increased levels of claudin-2 and exacerbated A549-Cl2 colonization. A direct effect of claudin dysregulation on colonization and the enhancement of EGF to this process have not been established and are reported here first.

Differences between A549 and MDCKII cells in the response to EGF and claudin-2 provide strong evidence for cell-specificity. EGF significantly triggers A549 cell remodeling and elevates claudin-2 levels in A549 cells. Prior studies report that EGF reduced claudin-2 levels in MDCKII cells [9]. The reason for these discrepancies are unclear but may be related to differences in cell origin, tumorigenicity, or occludin levels of expression as shown in this paper. Further research into NSCLC cell specificity is warranted.

These data must be interpreted in the context of the study design with the A549 cell serving as a model for a NSCLC tumor. In our experiments, while claudin-2 upregulation contributed to permeability differences and decreased inter-cellular adhesion we cannot ensure this phenotype results specifically from an increase in claudin-2 and not modification of claudin stoichometry or, in turn, abnormal claudin packaging in the TJ. Regardless, our data prove that deregulation of one claudin is sufficient to modify NSCLC physiology. Another caveat involves our measurements of TER and tracer permeability as units per area. While our data points were tight and reproducible we recognize irregular claudin-2 staining and A549 growth. As a result the effective area of the cell layer may vary. Cellular domes commonly found in AECs [49, 50] and identified in another NSCLC cell line [51] were also reported to constitute leaky areas of fluid transport. Moreover, in the latter study, dome regions were characterized by elevated surfactant and claudin-4 production. Together, these would contribute to aspects of the A549 cell barrier. Speculatively, properties of cell remodeling, loss of contact with the substratum, leaky fluid transport, and aberrant claudin expression could be enhanced by EGF action. Future studies on the relationship between EGF and claudin dysregulation in the context of NSCLC cells located within dome structures may lead to a more thorough understanding of regional tumor differences.

We show that in A549 cells EGF reduces permeability and induces reorganization. Inversely, EGFR inhibitors would restrain NSCLC remodeling and increase tumor permeabilization. NSCLC accounts for 80% of lung cancer deaths [52] and increased tumor exposure may help explain why combinations of angiostatins and EGFR inhibitors were reported to improve patient outcome [53,54].

In conclusion, EGF and claudin-2 pathways interact in the A549 cell. Unregulated growth can be modified by factors that affect paracellular permeability. Alternatively, agents that influence tumor permeability affect not only drug delivery, but also colonization. Understanding the link

between cell permeability and colonization will open the door for the development of novel antimetastatic agents.

Abbreviations

EGF, epidermal growth factor; MAPK, MAP kinase; EGFR, EGF receptor; TJs, tight junctions; AECs, alveolar epithelial cells; MDCKII, Madin Darby Canine Kidney Type II; TER, trans-epithelial resistance; NSCLC, non-small cell lung cancer.

ACKNOWLEDGMENTS

The authors would like to thank Jacob I. Sznajder and Daniel Tschumperlin for their assistance with this manuscript. This work was supported by NIH grant HL 007633 (YP) and YCIA from FAMRI (EL).

REFERENCES

1. Weinstat-Saslow D, Steeg PS. Angiogenesis and colonization in the tumor metastatic process: Basic and applied advances. FASEB J 1994;8:401–407. [PubMed: 7513289]
2. Lin MI, Yu J, Murata T, Sessa WC. Caveolin-1-deficient mice have increased tumor microvascular permeability, angiogenesis, and growth. Cancer Res 2007;67:2849–2856. [PubMed: 17363608]
3. Chen J, Somanath PR, Razorenova O, et al. Akt1 regulates pathological angiogenesis, vascular maturation and permeability in vivo. Nat Med 2005;11:1188–1196. [PubMed: 16227992]
4. Hoelting T, Siperstein AE, Clark OH, Duh QY. Epidermal growth factor enhances proliferation, migration, and invasion of follicular and papillary thyroid cancer in vitro and in vivo. J Clin Endocrinol Metab 1994;79:401–408. [PubMed: 8045955]
5. Meert AP, Verdebout JM, Martin B, Ninane V, Feoli F, Sculier JP. Epidermal growth factor receptor expression in preinvasive and early invasive bronchial lesions. Eur Respir J 2003;21:611–615. [PubMed: 12762344]
6. Borok Z, Hami A, Danto SI, Lubman RL, Kim KJ, Crandall ED. Effects of EGF on alveolar epithelial junctional permeability and active sodium transport. Am J Physiol 1996;270:L559–L565. [PubMed: 8928815]
7. Lipschutz JH, Li S, Arisco A, Balkovetz DF. Extracellular signal-regulated kinases 1/2 control claudin-2 expression in Madin-Darby canine kidney strain I and II cells. J Biol Chem 2005;280:3780–3788. [PubMed: 15569684]
8. Singh AB, Harris RC. Epidermal growth factor receptor activation differentially regulates claudin expression and enhances transepithelial resistance in Madin-Darby canine kidney cells. J Biol Chem 2004;279:3543–3552. [PubMed: 14593119]
9. Singh AB, Sugimoto K, Dhawan P, Harris RC. Juxtacrine activation of EGFR regulates claudin expression and increases transepithelial resistance. Am J Physiol Cell Physiol 2007;293:C1660–C1668. [PubMed: 17855771]
10. Singh AB, Sugimoto K, Harris RC. Juxtacrine activation of epidermal growth factor (EGF) receptor by membrane-anchored heparin-binding EGF-like growth factor protects epithelial cells from anoikis while maintaining an epithelial phenotype. J Biol Chem 2007;282:32890–32901. [PubMed: 17848576]
11. Vermeer PD, Einwalter LA, Moninger TO, et al. Segregation of receptor and ligand regulates activation of epithelial growth factor receptor. Nature 2003;422:322–326. [PubMed: 12646923]
12. Sakai K, Arao T, Shimoyama T, et al. Dimerization and the signal transduction pathway of a small in-frame deletion in the epidermal growth factor receptor. FASEB J 2006;20:311–313. [PubMed: 16373402]
13. Al Moustafa AE, Yen L, Benlimame N, Alaoui-Jamali MA. Regulation of E-cadherin/catenin complex patterns by epidermal growth factor receptor modulation in human lung cancer cells. Lung Cancer 2002;37:49–56. [PubMed: 12057867]
14. Tang VW, Goodenough DA. Paracellular ion channel at the tight junction. Biophys J 2003;84:1660–1673. [PubMed: 12609869]

15. Furuse M, Sasaki H, Fujimoto K, Tsukita S. A single gene product, claudin-1 or -2, reconstitutes tight junction strands and recruits occludin in fibroblasts. J Cell Biol 1998;143:391–401. [PubMed: 9786950]

16. Peter Y, Goodenough D. Claudins. Curr Biol 2004;14:R293–R294. [PubMed: 15084294]

17. Jeansonne B, Lu Q, Goodenough DA, Chen YH. Claudin-8 interacts with multi-PDZ domain protein 1 (MUPP1) and reduces paracellular conductance in epithelial cells. Cell Mol Biol (Noisy-le-grand) 2003;49:13–21. [PubMed: 12839333]

18. Hamazaki Y, Itoh M, Sasaki H, Furuse M, Tsukita S. Multi-PDZ domain protein 1 (MUPP1) is concentrated at tight junctions through its possible interaction with claudin-1 and junctional adhesion molecule. J Biol Chem 2002;277:455–461. [PubMed: 11689568]

19. Chen SP, Zhou B, Willis BC, et al. Effects of transdifferentiation and EGF on claudin isoform expression in alveolar epithelial cells. J Appl Physiol 2005;98:322–328. [PubMed: 15361518]

20. Wang F, Daugherty B, Keise LL, et al. Heterogeneity of claudin expression by alveolar epithelial cells. Am J Respir Cell Mol Biol 2003;29:62–70. [PubMed: 12600828]

21. Daugherty BL, Mateescu M, Patel AS, et al. Developmental regulation of claudin localization by fetal alveolar epithelial cells. Am J Physiol Lung Cell Mol Physiol 2004;287:L1266–L1273. [PubMed: 15347569]

22. Guillemot L, Citi S. Cingulin regulates claudin-2 expression and cell proliferation through the small GTPase RhoA. Mol Biol Cell 2006;17:3569–3577. [PubMed: 16723500]

23. Van Itallie CM, Fanning AS, Anderson JM. Reversal of charge selectivity in cation or anion-selective epithelial lines by expression of different claudins. Am J Physiol Renal Physiol 2003;285:F1078–F1084. [PubMed: 13129853]

24. Amasheh S, Meiri N, Gitter AH, et al. Claudin-2 expression induces cation-selective channels in tight junctions of epithelial cells. J Cell Sci 2002;115:4969–4976. [PubMed: 12432083]

25. Furuse M, Furuse K, Sasaki H, Tsukita S. Conversion of zonulae occludentes from tight to leaky strand type by introducing claudin-2 into Madin-Darby canine kidney I cells. J Cell Biol 2001;153:263–272. [PubMed: 11309408]

26. Kobayashi S, Kondo S, Juni K. Permeability of peptides and proteins in human cultured alveolar A549 cell monolayer. Pharm Res 1995;12:1115–1119. [PubMed: 7494821]

27. Kusama T, Mukai M, Tatsuta M, Matsumoto Y, Nakamura H, Inoue M. Selective inhibition of cancer cell invasion by a geranylgeranyltransferase-I inhibitor. Clin Exp Metastasis 2003;20:561–567. [PubMed: 14598891]

28. Peter Y, Rotman G, Lotem J, Elson A, Shiloh Y, Groner Y. Elevated Cu/Zn-SOD exacerbates radiation sensitivity and hematopoietic abnormalities of Atm-deficient mice. EMBO J 2001;20:1538–1546. [PubMed: 11285218]

29. Grande M, Franzen A, Karlsson JO, Ericson LE, Heldin NE, Nilsson M. Transforming growth factor-beta and epidermal growth factor synergistically stimulate epithelial to mesenchymal transition (EMT) through a MEK-dependent mechanism in primary cultured pig thyrocytes. J Cell Sci 2002;115:4227–4236. [PubMed: 12376555]

30. Gazdar AF, Shigematsu H, Herz J, Minna JD. Mutations and addiction to EGFR: The Achilles 'heal' of lung cancers? Trends Mol Med 2004;10:481–486. [PubMed: 15464447]

31. Lan M, Kojima T, Osanai M, Chiba H, Sawada N. Oncogenic Raf-1 regulates epithelial to mesenchymal transition via distinct signal transduction pathways in an immortalized mouse hepatic cell line. Carcinogenesis 2004;25:2385–2395. [PubMed: 15308585]

32. Stevenson BR, Siliciano JD, Mooseker MS, Goodenough DA. Identification of ZO-1: A high molecular weight polypeptide associated with the tight junction (zonula occludens) in a variety of epithelia. J Cell Biol 1986;103:755–766. [PubMed: 3528172]

33. Denker BM, Nigam SK. Molecular structure and assembly of the tight junction. Am J Physiol 1998;274:F1–F9. [PubMed: 9458817]

34. Anderson JM, Van Itallie CM, Peterson MD, Stevenson BR, Carew EA, Mooseker MS. ZO-1 mRNA and protein expression during tight junction assembly in Caco-2 cells. J Cell Biol 1989;109:1047–1056. [PubMed: 2670954]

35. Siliciano JD, Goodenough DA. Localization of the tight junction protein, ZO-1, is modulated by extracellular calcium and cell-cell contact in Madin-Darby canine kidney epithelial cells. J Cell Biol 1988;107:2389–2399. [PubMed: 3058722]
36. Flores-Benitez D, Ruiz-Cabrera A, Flores-Maldonado C, Shoshani L, Cereijido M, Contreras RG. Control of tight junctional sealing: Role of epidermal growth factor. Am J Physiol Renal Physiol 2006;292:F828–F836. [PubMed: 17077385]
37. Lichtner RB, Kaufmann AM, Kittmann A, et al. Ligand mediated activation of ectopic EGF receptor promotes matrix protein adhesion and lung colonization of rat mammary adenocarcinoma cells. Oncogene 1995;10:1823–1832. [PubMed: 7753557]
38. Michl P, Barth C, Buchholz M, et al. Claudin-4 expression decreases invasiveness and metastatic potential of pancreatic cancer. Cancer Res 2003;63:6265–6271. [PubMed: 14559813]
39. Kim KJ, Borok Z, Ehrhardt C, Willis BC, Lehr CM, Crandall ED. Estimation of paracellular conductance of primary rat alveolar epithelial cell monolayers. J Appl Physiol 2005;98:138–143. [PubMed: 15273240]
40. Matthay MA, Folkesson HG, Clerici C. Lung epithelial fluid transport and the resolution of pulmonary edema. Physiol Rev 2002;82:569–600. [PubMed: 12087129]
41. Lazrak A, Samanta A, Matalon S. Biophysical properties and molecular characterization of amiloride-sensitive sodium channels in A549 cells. Am J Physiol Lung Cell Mol Physiol 2000;278:L848–L857. [PubMed: 10749763]
42. Peter Y. Tracheotomy: A method for transplantation of stem cells to the lung. J Vis Experimentation 2007;2:163.
43. Warburton D, Schwarz M, Tefft D, Flores-Delgado G, Anderson KD, Cardoso WV. The molecular basis of lung morphogenesis. Mech Dev 2000;92:55–81. [PubMed: 10704888]
44. Wu Z, Yang L, Cai L, et al. Detection of epithelial to mesenchymal transition in airways of a bleomycin induced pulmonary fibrosis model derived from an alpha-smooth muscle actin-Cre transgenic mouse. Respir Res 2007;8:1. [PubMed: 17207287]
45. Khoury H, Naujokas MA, Zuo D, et al. HGF converts ErbB2/Neu epithelial morphogenesis to cell invasion. Mol Biol Cell 2005;16:550–561. [PubMed: 15548598]
46. Kinugasa T, Sakaguchi T, Gu X, Reinecker HC. Claudins regulate the intestinal barrier in response to immune mediators. Gastroenterology 2000;118:1001–1011. [PubMed: 10833473]
47. Morin PJ. Claudin proteins in human cancer: Promising new targets for diagnosis and therapy. Cancer Res 2005;65:9603–9606. [PubMed: 16266975]
48. Ben-Yosef T, Belyantseva IA, Saunders TL, et al. Claudin 14 knockout mice, a model for autosomal recessive deafness DFNB29, are deaf due to cochlear hair cell degeneration. Hum Mol Genet 2003;12:2049–2061. [PubMed: 12913076]
49. Sugahara K, Caldwell JH, Mason RJ. Electrical currents flow out of domes formed by cultured epithelial cells. J Cell Biol 1984;99:1541–1544. [PubMed: 6480702]
50. Mason RJ, Williams MC, Widdicombe JH, Sanders MJ, Misfeldt DS, Berry LC Jr. Transepithelial transport by pulmonary alveolar type II cells in primary culture. Proc Natl Acad Sci USA 1982;79:6033–6037. [PubMed: 6964398]
51. Shlyonsky V, Goolaerts A, Van Beneden R, Sariban-Sohraby S. Differentiation of epithelial Na+ channel function. An in vitro model. J Biol Chem 2005;280:24181–24187.
52. Wingo, PA.; Ries, LA.; Giovino, GA., et al. Annual report to the nation on the status of cancer, 1973–1996. with a special section on lung cancer and tobacco smoking; J Natl Cancer Inst. 1999. p. 675-690. [see comment]
53. Haber DA, Bell DW, Sordella R, et al. Molecular targeted therapy of lung cancer: EGFR mutations and response to EGFR inhibitors. Cold Spring Harb Symp Quant Biol 2005;70:419–426. [PubMed: 16869779]
54. Cabebe E, Wakelee H. Role of anti-angiogenesis agents in treating NSCLC: Focus on bevacizumab and VEGFR tyrosine kinase inhibitors. Curr Treat Options Oncol 2007;8:15–27. [PubMed: 17634832]

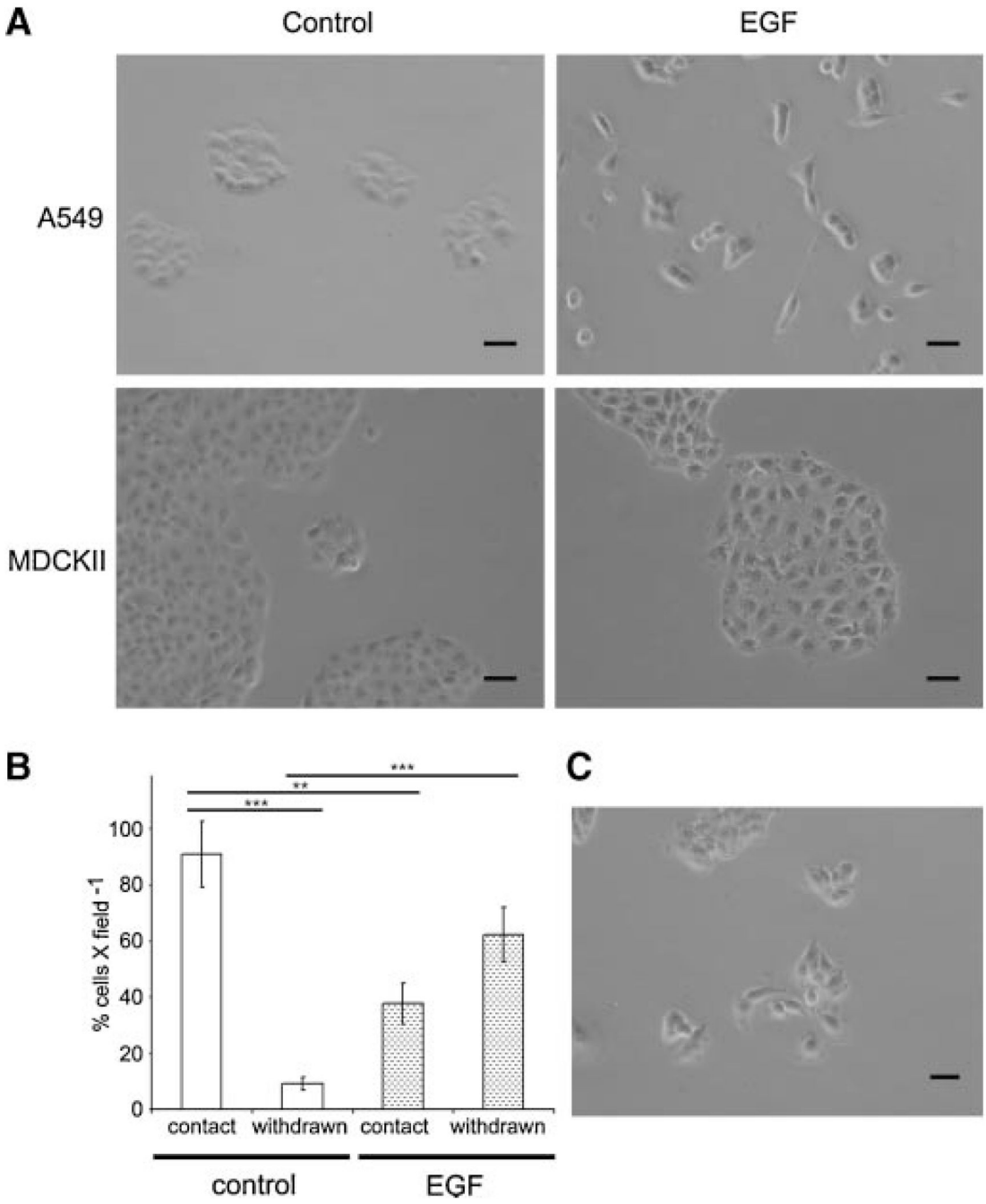

Figure 1. EGF induced A549 cell reorganization is reversed by MAPK inhibition

(A) 1×10^5 A549 (upper) and MDCKII (lower) cells were plated and incubated for 3 d in vehicle (control; left) and EGF (right). (B) Histogram depicting the total number of cells within cellular foci (contact; with at least two neighboring cells) or cells withdrawn from the focus. (C) EGF administered A549 cells pretreated with PD98059 are similar to controls. Statistically significant with $^{**}P < 0.01$, and $^{***}P < 0.001$. Scale bar = 20 μm.

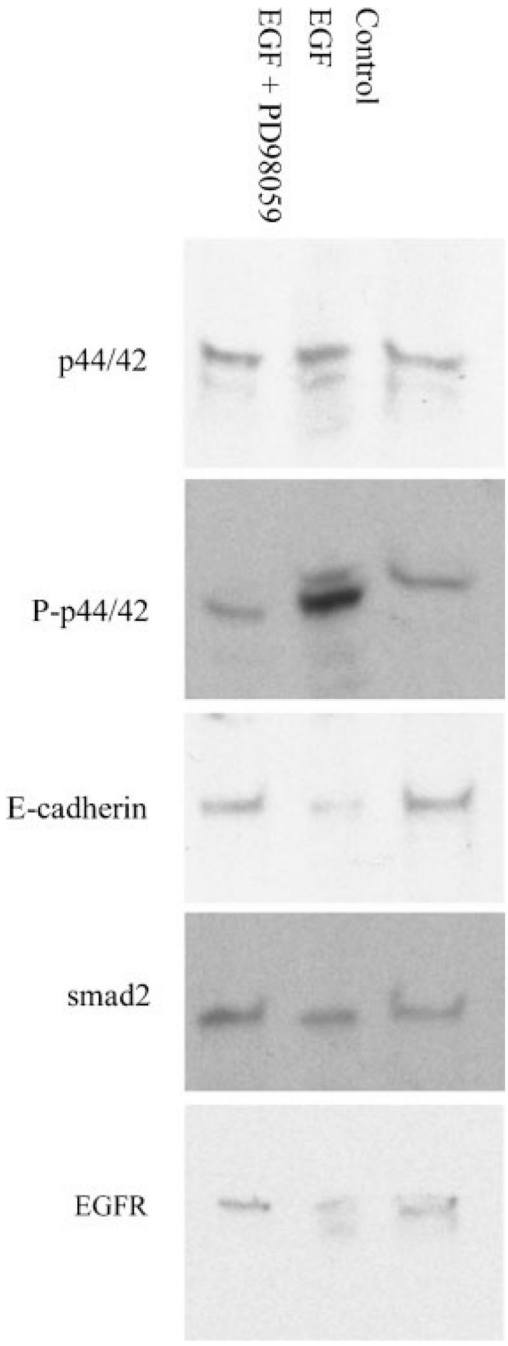

Figure 2. MAPK mediates the downstream affect of EGF in A549 cells

Western blot analysis of the EGFR, MAPK (p44/42), phosphorylated MAPK (P-p44/42), E-cadherin, and smad-2, in lysates of A549 cells treated with EGF (200 ng/mL) or EGF and PD98059 (50 μM). Seventy micrograms of protein was loaded per well. In EGF treated A549 cells, the increase in phosphorylated MAPK signal is reversed by pretreatment with PD98059.

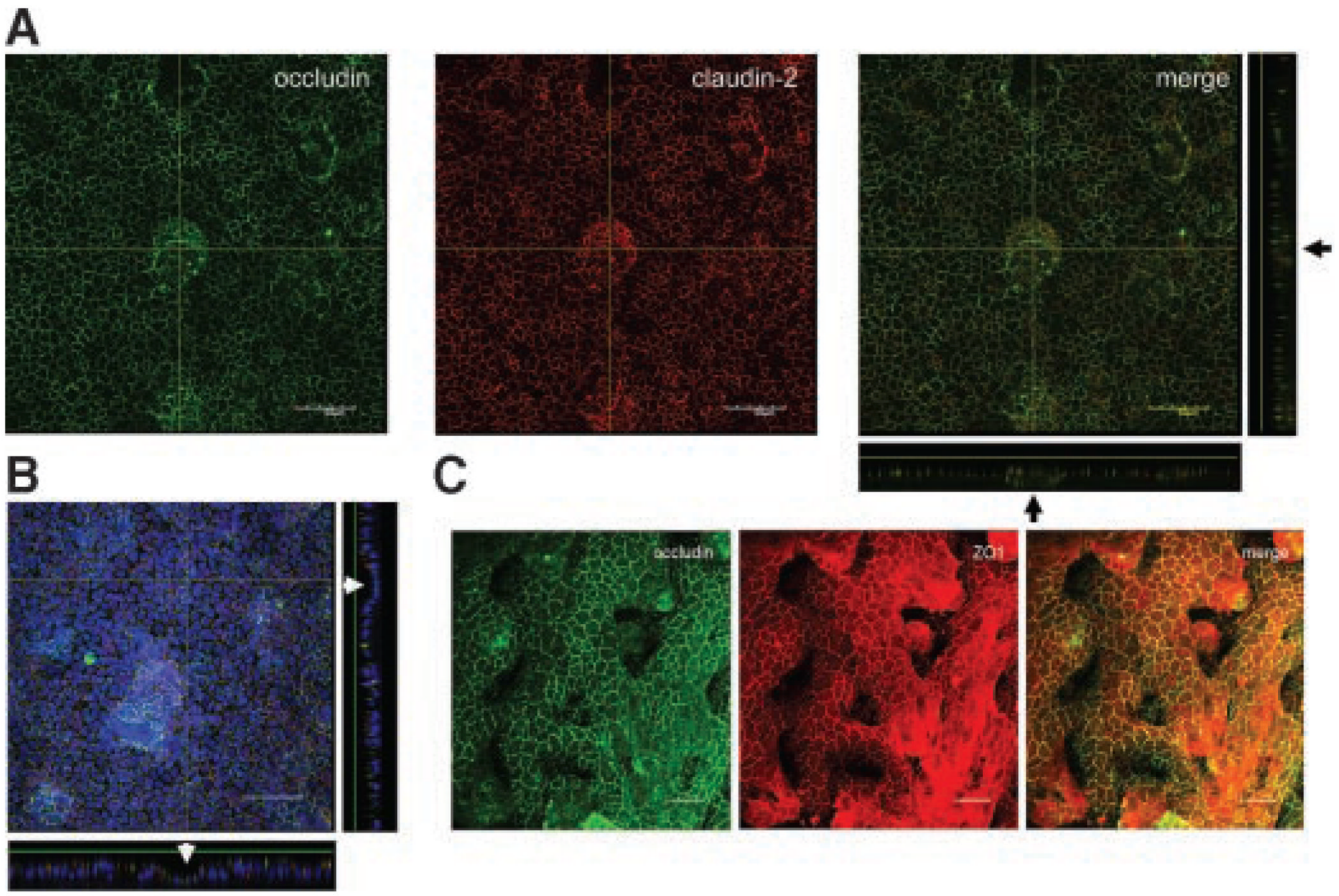

Figure 3. A549 cells display convoluted growth and laterally express TJ proteins

Cells were grown on a transwell insert, stained for TJ proteins and prepared for confocal microscopy. (A) Lateral localization of occludin and claudin-2 with the appropriate sections shown on the bottom and right aspects. Note that the central upgrowth is comprised of a double cellular layer, black arrows. (B) In contrast, occludin and claudin-2 staining demonstrate a dome structure as observed by sections on the bottom and right aspects (white arrows). Blue represents DAPI counterstain for nuclei. Scale bar = 50 μm. (C) Single section through an A549 layer double-stained for occludin (green) and ZO1 (red) demonstrates complex cell growth. Dark areas result from lack of proteins at this level. Scale bar = 20 μm.

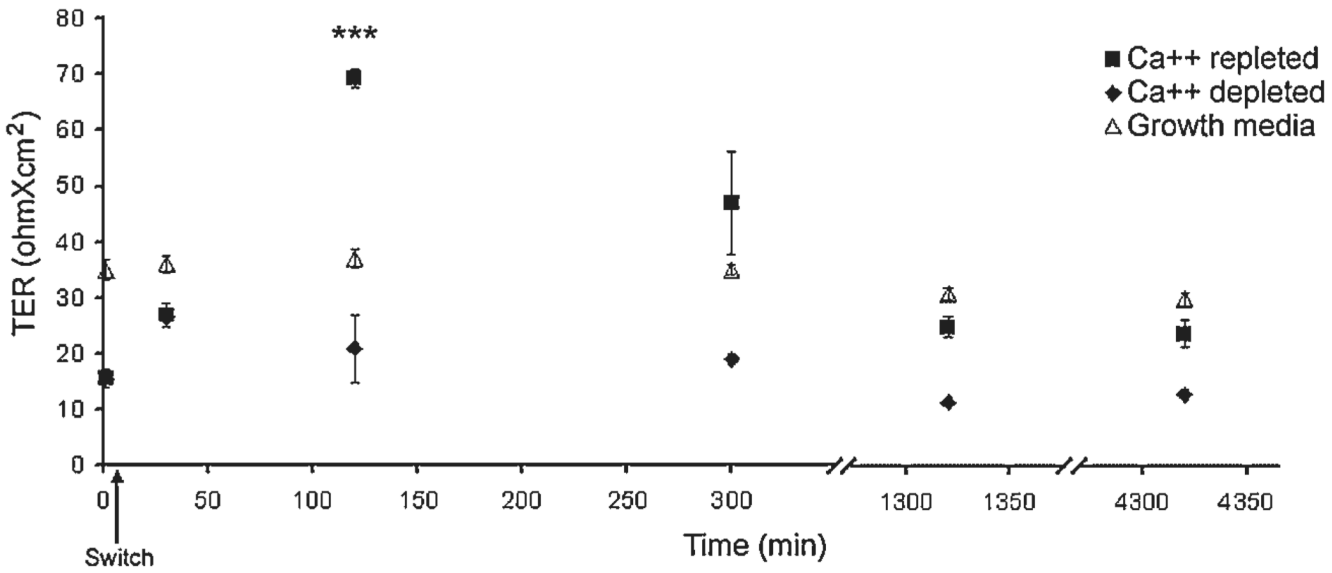

Figure 4. Ca++ dependent TER in A549 cells

A549 cells grown on transwell inserts in growth and Ca++ depleted media for 1 wk. The latter was then replaced for growth media and TER was measured for all groups at the designated time points. Arrow indicates switch back to growth (calcium containing) media.
***Statistically significant at $P < 0.001$.

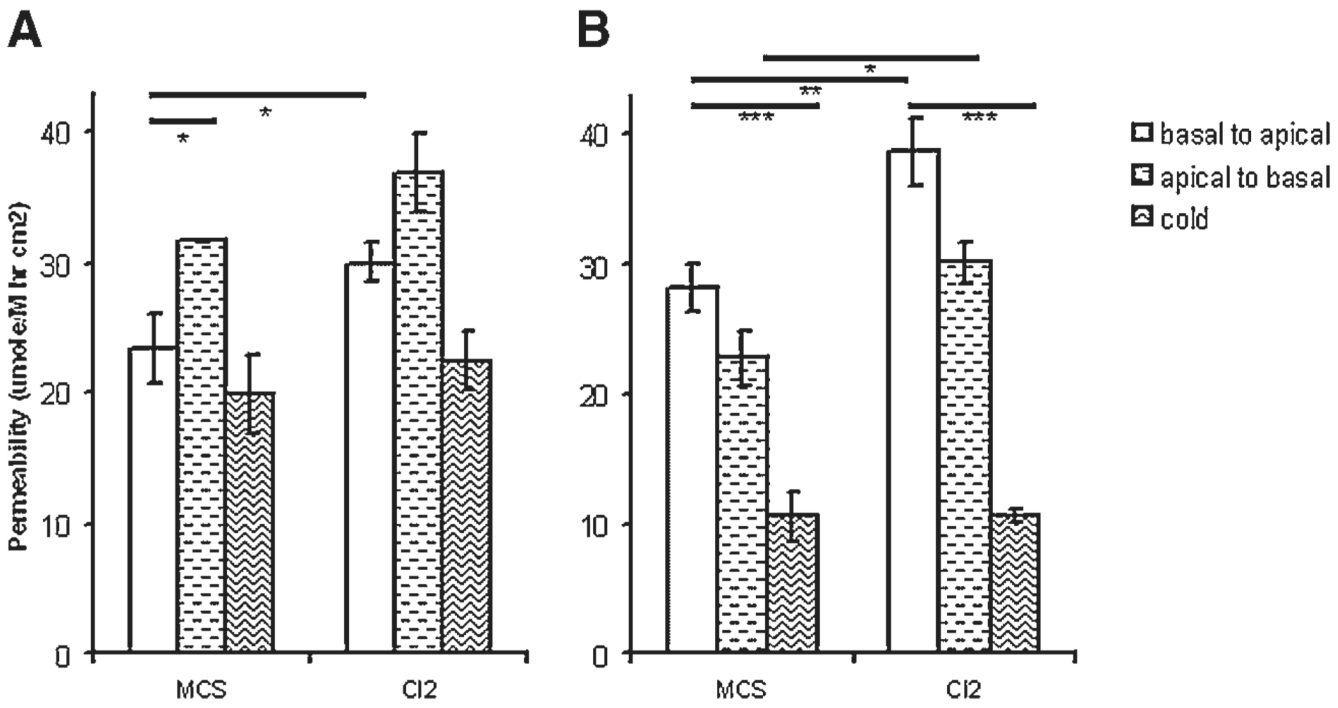

Figure 5. A549 permeability is modified by claudin-2 overexpression

A549 cells were grown for 3 wk on a transwell insert and permeability to ethanolamine and mannitol are shown. (A) Ethanolamine permeability is significantly higher in the apical to basal direction and enhanced as a result of claudin-2 overexpression. (B) Mannitol permeability is temperature sensitive and increased as a result of claudin-2 upregulation. MCS, empty vector control; Cl2, claudin-2 overexpressing cells. Statistically significant by *t*-test with $*P < 0.05$, $**P < 0.01$, and $***P < 0.001$.

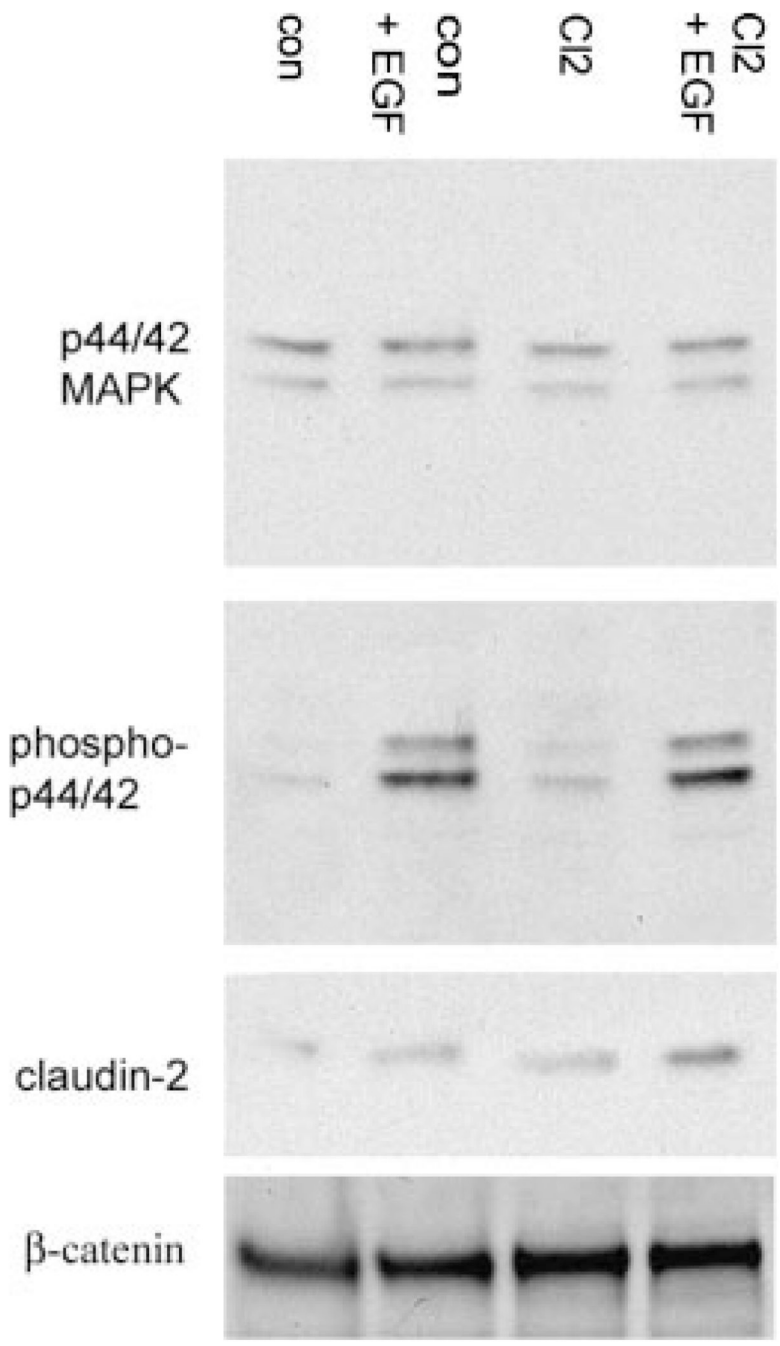

Figure 6. Claudin-2 levels are elevated in EGF treated A549 cells

A549 cells were treated with EGF for 24 h and equal amounts of protein were analyzed for claudin-2, MAPK, phospho-MAPK, and β-catenin expression. Both A549-con and A549-Cl2 cells exhibit increased levels of claudin-2 protein following EGF treatment.

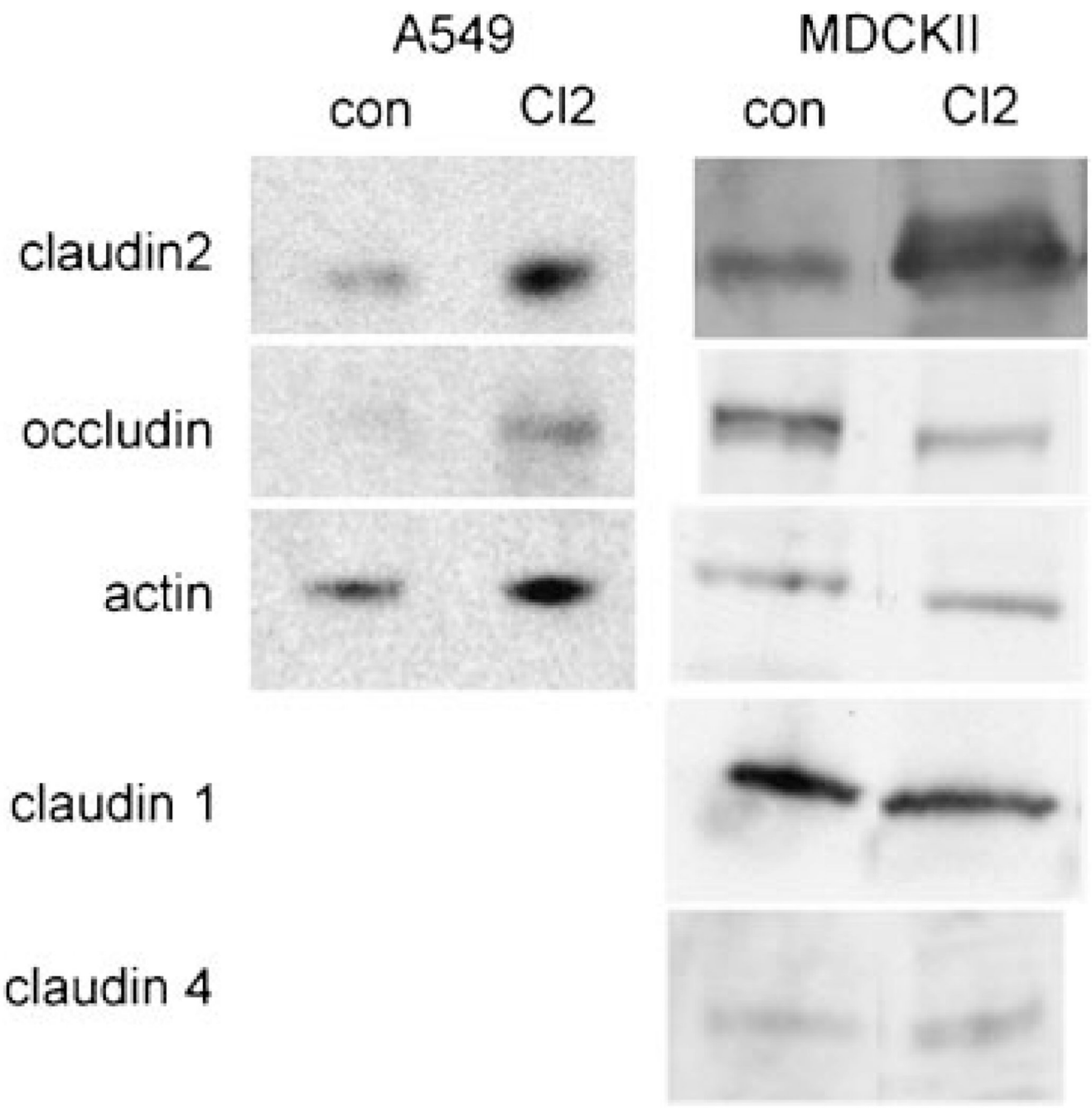

Figure 7. Claudin-2 overexpression in the A549 cell

Western blot depicts cellular protein levels (70 μg protein per well) of stably transfected empty vector (con) and claudin-2 (Cl2) A549 and MDCKII cells, respectively. A549 cells do not express claudin -1 or -4 and blots are not shown. Note differences in levels of occludin between claudin-2 overexpressing cells and their respective controls ($n \geq 3$).

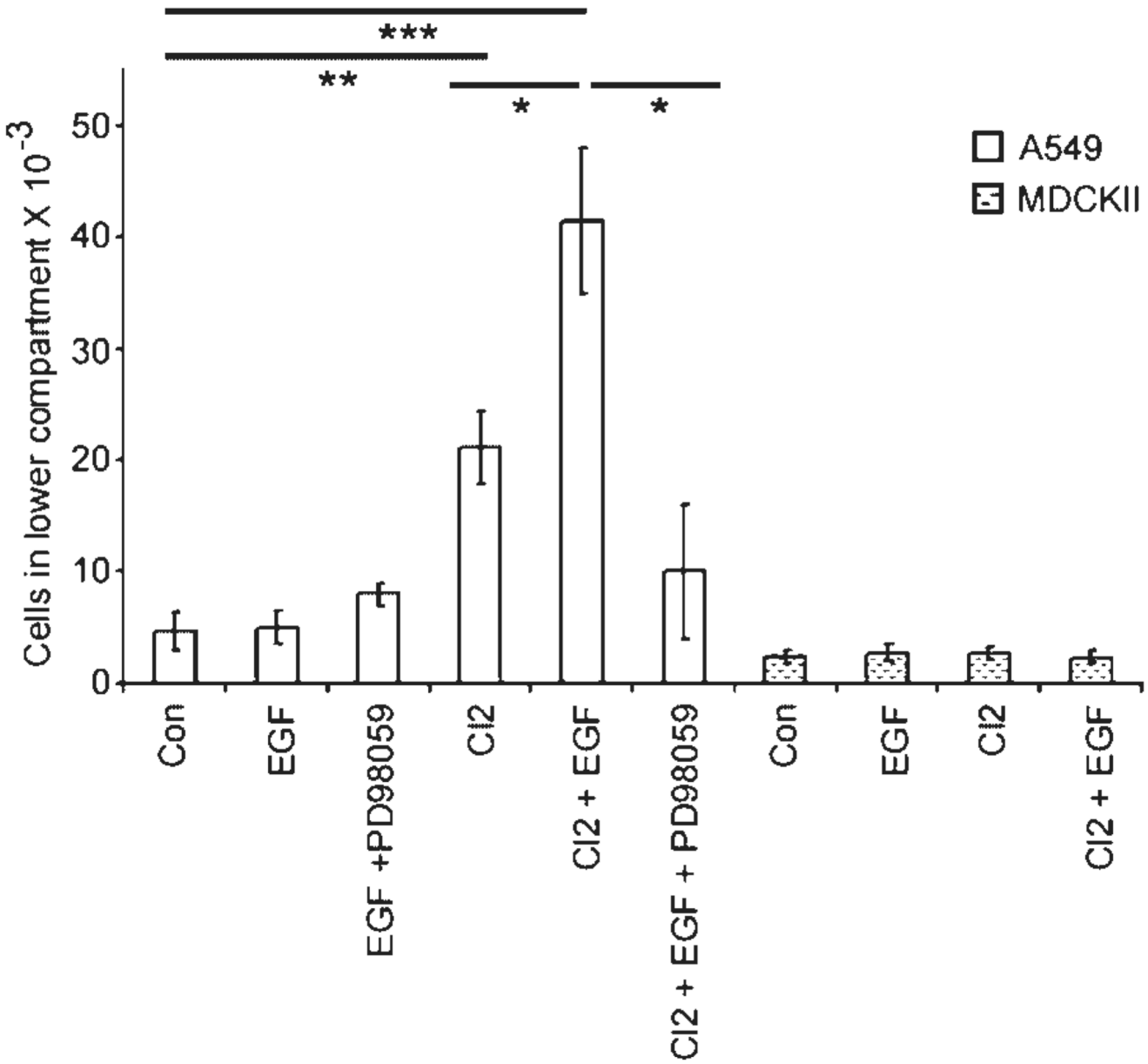

Figure 8. EGF and claudin-2 cooperate to increase A549 colonization

Cells grown to confluency in the upper chamber of a transwell insert were flooded with media for 3 d to allow colonization of cells in the lower well. A549-Cl2 show enhanced colonization as compared to controls. Treatment with EGF significantly increases this effect. MDCKII cells do not respond to either treatment. *$P < 0.05$, **$P < 0.01$, and ***$P < 0.001$.